

Received 18 November 2023, accepted 27 November 2023, date of publication 30 November 2023,  
date of current version 6 December 2023.

Digital Object Identifier 10.1109/ACCESS.2023.3338537

## RESEARCH ARTICLE

# A Real-Time Autonomous Gravity Measurement Method for Underwater Gravity-Aided Navigation

WENYU AI<sup>1,2,3</sup>, SHENG ZHONG<sup>1,2</sup>, YUE LENG<sup>1,2,3</sup>, AND SHIBO WANG<sup>1,3</sup>

<sup>1</sup>School of Artificial Intelligence and Automation, Huazhong University of Science and Technology, Wuhan 430074, China

<sup>2</sup>National Key Laboratory of Multispectral Information Intelligent Processing Technology, Huazhong University of Science and Technology, Wuhan 430074, China

<sup>3</sup>Wuhan National Laboratory for Optoelectronics, Huazhong Institute of Electro-Optics, Wuhan 430223, China

Corresponding author: Shibo Wang (shibowang@buaa.edu.cn)

**ABSTRACT** Underwater gravity-assisted navigation is typically employed by submarines as a navigation method when external navigation information is not easily available, which necessitates the acquisition of gravity information through autonomous measurement. However, underwater gravity measurement research currently relies heavily on high-precision external navigation information, such as acoustic positioning, and lacks autonomy. Therefore, there is a contradiction between the existing underwater gravity measurement technology and the underwater gravity-assisted navigation application scenario. To solve this problem, a real-time, autonomous gravity measurement method specifically designed for underwater gravity-assisted navigation is proposed in this study. The proposed method achieves real-time, autonomous underwater gravity measurement with mGal-level precision by integrating classical gravity measurement principles, which involves a gravimeter, an electromagnetic log (EML), and a depth gauge (DG). To evaluate the proposed method's effectiveness, a semi-physical simulation was conducted through vehicle testing. The experimental results demonstrated that the proposed method achieved a precision of 1.01 mGal at 0.0033 Hz within the repeated measuring line.

**INDEX TERMS** Gravimeter, autonomous gravity measurement, underwater, gravity-assisted navigation, integrated navigation.

## I. INTRODUCTION

The development of a high-precision global gravity field model is a fundamental research task in the field of geodesy, as it provides a fundamental method for addressing global issues, such as climate change, melting polar ice caps, rising sea levels, and geological disasters [1], [2]. Marine gravity measurement is a reliable and effective technique for enhancing the accuracy of gravity field models. It enables the rapid acquisition of high-resolution and high-precision gravity data and facilitates large-scale and efficient gravity measurements [3], [4]. Since the late 20th century, the field of marine gravity measurement has experienced significant growth, resulting in the development of various types of marine gravity instruments and technologies, such as the strapdown and platform types [5], [6], [7].

The associate editor coordinating the review of this manuscript and approving it for publication was Yougan Chen<sup>1</sup>.

In the last decade, there has been a growing demand for higher-resolution underwater short-wave gravity information to enhance the efficiency of deep-sea mineral exploration and the accuracy of seafloor topography inversion. Driven by practical requirements in oil and gas exploration and marine scientific research, marine gravity instruments have progressively extended their underwater measurement capabilities [8], [9]. Consequently, several research institutions are focusing on developing high-precision navigation and motion acceleration processing methods that are suitable for underwater gravity measurements. The University of Tokyo has adapted and enhanced the Micro-g LaCoste S-174 marine gravity instrument by integrating it with an Autonomous Underwater Vehicle (AUV) named Urashima. The AUV employs a depth gauge (DG) sensor to measure the vertical motion acceleration and combines the gravity instrument/Doppler Velocity Log (DVL) to offer navigation information. This approach delivers a high-precision

underwater gravity measurement accuracy of 0.1 mGal [10], [11]. The Institute of Marine Technology Problems in Russia has investigated underwater gravity measurement using an AUV equipped with a gravity instrument. They have integrated an on-board navigation system and a hydro-acoustic navigation system with a long-base to provide location information and employed multiple corrections from the sea surface Global Positioning System (GPS). Based on their findings, they have confirmed that the underwater gravity measurement accuracy achieved by an AUV-equipped gravity instrument is superior to the mGal level [12]. Wuhan University in China has researched data processing methods for underwater gravity measurement. They have introduced a continuous-discrete Kalman filter approach to integrate data from various sources, including gravity instruments, GPS, short baseline, DVL, and DG. This method delivers navigation information that satisfies the demands of underwater gravity measurement [13]. The National University of Defense Technology in China has developed an integrated system that includes a gravity instrument, DG, and DVL to provide navigation information and vertical motion acceleration data for underwater gravity measurement. With this system, they have achieved a high accuracy of 1.06 mGal [14]. Moreover, to ensure navigation performance in the event of a complete loss of DVL, they have introduced a carrier trajectory constraint. This constraint can be used as observation information for integrated navigation, ensuring that navigation information can be used for gravity measurement related corrections, ultimately achieving underwater gravity measurement accuracy of 2.03 mGal [15].

Currently, the accuracy of underwater gravity measurement is comparable to that of traditional on-surface scenarios, which is sufficient for gravity mapping and resource exploration. The technology and databases for underwater gravity measurement are continually evolving and improving [16], [17], [18], which has created the necessary conditions for autonomous navigation based on underwater inertial/gravity matching. Numerous scholars have investigated autonomous navigation algorithms based on inertial/gravity matching [19], [20], [21]. In military applications, autonomous navigation based on underwater inertial/gravity matching is an essential technique for large and medium-sized underwater vehicles, submarines, and other platforms to achieve extended and covert navigation as a passive navigation technology. However, the application of underwater inertial/gravity matching navigation imposes very high requirements on the autonomy of gravity measurement [22]. Currently, underwater gravity measurement primarily focuses on gravity field mapping and relies on auxiliary methods, such as DVL, acoustic positioning, or even mother ship towing. These methods require the outward emission of signals or the pre-deployment of signal response base stations, resulting in a lack of autonomy. Consequently, current underwater gravity measurement methods are inadequate to meet the requirements of autonomous navigation based on underwater inertial/gravity matching.

This study proposes a novel, real-time autonomous method for gravity measurement in underwater gravity-assisted navigation to address the aforementioned issues. The proposed method involves a fusion of data from the gravity instrument, electromagnetic log (EML), and DG to obtain comprehensive information about the underwater environment. This information includes depth, motion acceleration, velocity, position, and attitude, which are essential for autonomous navigation based on underwater inertial/gravity matching. This study provides a comprehensive exposition of the proposed method and conducted semi-physical simulation verification using onboard test data to validate its effectiveness. The study's innovations are summarized as follows:

(1) An underwater autonomous gravity measurement method based on the fusion data from the gravity instrument, EML, and DG was proposed in response to the requirements of underwater gravity-assisted autonomous navigation.

(2) A depth information processing method based on the fusion of data from the gravity instrument and DG was developed to enhance the accuracy of vertical motion acceleration acquisition by the carrier and fulfill the demands of underwater autonomous gravity measurement for depth information and motion acceleration information.

(3) To meet the requirements of underwater autonomous gravity measurement for navigation information, such as position and velocity, a gravity instrument and EML fusion navigation method based on adaptive delay state filtering of measurement noise were proposed. This method effectively suppresses the effects of water flow velocity and sensor noise on EML measurement accuracy.

## II. REAL-TIME UNDERWATER AUTONOMOUS GRAVITY MEASUREMENT METHOD BASED ON THE FUSION OF GRAVITY INSTRUMENT/EML/DG

### A. THE PROPOSED GRAVITY MEASUREMENT METHOD AT A GLANCE

This study outlines a real-time underwater autonomous gravity measurement method based on the fusion of gravity instrument/EML/DG. The method comprises of three main parts: an inertial navigation solution, data fusion, and a gravity solution. In the inertial navigation solution, the initial navigation information was determined by using the carrier's motion data obtained from the gyroscope and accelerometer. The inertial measurement data was projected onto the horizontal plane in the geodetic coordinate system based on the heading and attitude information, and data integration yields the navigation information of heading, attitude, velocity, and position. The data fusion process involves combining information from the gravity instrument/DG and the gravity instrument/EML. The former provided depth information and vertical motion acceleration information, while the latter provided navigation information, such as position, velocity, and attitude. In the gravity solution, the motion acceleration and gravity acceleration of the carrier were determined based on the equation of motion using navigation information, depth information, and inertial measurement data as inputs.

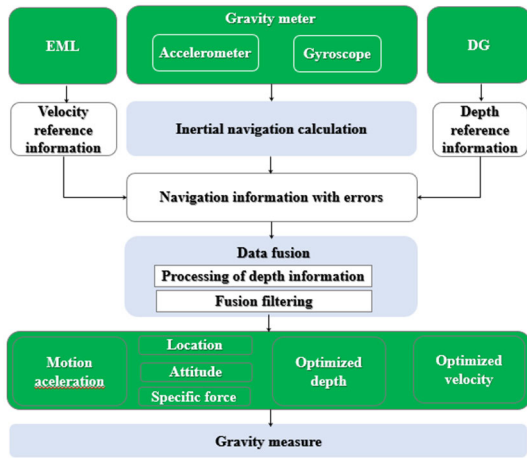


**FIGURE 1.** A real-time underwater autonomous gravity measurement method based on the fusion of gravity instrument/EML/DG.

Low-frequency gravity measurement results were obtained through data processing techniques like low-pass filtering. The data processing flow is illustrated in the figure 1.

Gravity instruments typically incorporate an integrated gyroscope and accelerometer to measure inertial data, such as specific force and angular velocity. This data is used to obtain inertial navigation solutions and acquire navigation information, which may contain errors. The depth reference information is obtained from the DG, while the EML provides velocity reference information. These measurements are fused with the navigation information containing errors to determine high-precision navigation information, including high-precision motion acceleration and attitude. The gravity solution is obtained by utilizing specific force data and high-precision navigation information as inputs. Inertial navigation solutions and gravity solutions are well-established and have been extensively researched by several scholars [23], [24], and thus will not be elaborated further in this study. Instead, our focus is on the data fusion segment, where we merge data from the gravity instrument, EML, and DG to deliver a solution that meets the requirements of autonomous underwater gravity measurement. The fundamental data processing expression is expressed as follows:

$$g = -C_b^n f + a + E \tag{1}$$

In the above equations,  $g$  denotes the gravity measurement result,  $C_b^n$  represents the attitude transfer matrix from the gravity instrument coordinate system to the geographic coordinate system, which is determined by the carrier's attitude information,  $f$  denotes the specific force information, which is measured by the gravity instrument's built-in accelerometer,  $a$  represents the vertical motion acceleration of the carrier, which is obtained after processing the depth information, and  $E$  denotes the sum of the Eötvös effect and normal gravity, which is determined by the position, depth, and velocity. To enhance the accuracy of autonomous underwater gravity measurement, two critical factors must be considered:

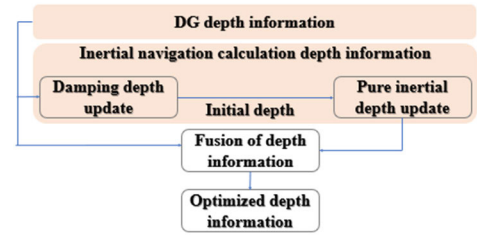


**FIGURE 2.** Depth information processing method based on the fusion of gravity instrument/DG.

(1) Improving the measurement accuracy of the carrier's vertical motion acceleration: The accuracy of the vertical motion acceleration, computed by performing depth information double differentiation, is subject to the noise level and stability of the depth measurement information.

(2) Improving the accuracy of the carrier's velocity, position, and depth measurements: Velocity, position, and depth information are crucial for extracting the gravity measurement results and are essential for correcting the Eötvös effect and normal gravity during gravity calculation.

After obtaining the carrier navigation information, the steps to achieve gravity measurement are as follows: 1) The acceleration information is measured by the internal sensors of the gravimeter. 2) Using attitude information to project acceleration information, obtain vertical specific force information. 3) Second order differential depth information is used to obtain the vertical motion acceleration of the carrier. 4) Perform secondary differential calculation on the elevation information to obtain the vertical motion acceleration of the carrier. 5) According to Newton's Second Law, combined with the calculation results of Coriolis acceleration, centripetal acceleration, and vertical motion acceleration, the decoupling of vertical specific force information and gravity information is completed to obtain unfiltered gravity information. 6) Design a Hann window FIR low-pass filter with a filtering window of 300s, a passband cutoff frequency of 0.0033Hz (attenuation gain of  $-3\text{dB}$ ), and a stopband attenuation gain of less than  $-80\text{dB}$ . 5) Using FIR low-pass filter to process unfiltered gravity information and obtain gravity measurement results. The detailed analytical formula for the above steps can be found in references [23], [24].

**B. DEPTH INFORMATION PROCESSING METHOD BASED ON THE FUSION OF GRAVITY INSTRUMENT/DG**

Depth gauge measures depth by using water pressure, and commercial products can achieve a depth measurement accuracy of  $\pm 0.015\%$  FS (where FS refers to the water depth at the carrier's location) [25]. This feature enables DG to provide depth reference information for autonomous underwater gravity measurement [11]. To improve the accuracy and stability of depth information, this study integrates depth information from two sources: inertial navigation and DG. The integrated approach considers the carrier's motion state and ensures that the depth information is smooth and continuous, enhancing the accuracy of the carrier's vertical motion

acceleration calculation. Inertial navigation calculates depth information with short-term high precision, continuity, and high bandwidth. In contrast, DG depth information has good long-term stability but lower data frequency. The data processing flowchart is illustrated in the figure 2.

Inertial navigation-calculated depth consists of damping depth and pure inertial depth, which are obtained through two independent depth calculation channels: inertial navigation depth channel 1 and inertial navigation depth channel 2. Inertial navigation depth channel 1 uses a second-order damping network [26] to calculate depth error with DG depth information as the reference value. The depth error is then introduced into the update loop of inertial navigation depth channel 1 through a proportional link, and the error is compensated for in the vertical velocity and acceleration to obtain the damping depth. Inertial navigation depth channel 2 is based on the specific force equation and performs pure inertial open-loop depth updating based on velocity integration. The initial value of inertial navigation depth channel 2 is continuously updated by inertial navigation depth channel 1.

To integrate the depth information calculated by inertial navigation and DG, a depth fusion factor is constructed based on the carrier's motion state. The carrier's motion state includes both instantaneous and long-term motion states. The instantaneous motion state describes the peak value  $q_b$  of the carrier's vertical motion acceleration over a period of time, while the long-term motion state describes the standard deviation  $s_b$  of the carrier's vertical motion acceleration over a period of time. The depth fusion factor is formulated as follows:

$$p_b = 1 - s_b q_b / Th \quad (2)$$

The equations above include a threshold  $Th$  for determining the carrier's motion, which is calculated as the maximum absolute value of the product of  $q_b$  and  $s_b$  of the carrier's vertical motion acceleration during normal navigation. Using the depth fusion factor, the depth information result  $h_{acc}$  can be obtained as follows:

$$h_{acc} = p_b h_{sin s} + (1 - p_b) h_{dg} \quad (3)$$

The equations above involve  $h_{dg}$ , which represents the DG depth information, and  $h_{sin s}$ , which represents the inertial navigation depth information. When the carrier performs altitude maneuvers, the response speed of  $h_{dg}$  is limited, causing an increase in the weight of  $h_{sin s}$ . The differential value  $h_{acc}$  can be obtained from the carrier's vertical motion acceleration.

### C. GRAVITY METER/EML FUSION NAVIGATION METHOD BASED ON ADAPTIVE DELAY STATE FILTERING FOR MEASUREMENT NOISE

The EML measures water velocity using the electromagnetic induction law and can achieve a measurement accuracy of  $\pm 0.2$  knot when the ship's speed is less than 10knot [27]. It provides a stable and reliable speed reference for

autonomous underwater gravity measurement. However, the EML measurement speed is not equivalent to ground speed and can be influenced by water flow factors. Therefore, it cannot be directly integrated into the gravity meter/EML fusion. This study proposes a gravity meter/EML fusion method based on adaptive delay state filtering, which considers the unique characteristics of EML and the requirements for underwater gravity measurement. The state equation of the proposed method uses the error model of the inertial navigation system, while the observation equation uses the differential water velocity provided by EML. To mitigate the effect of water flow velocity, a measurement equation that includes a delay state is constructed. Furthermore, the measurement noise adaptive delay state filtering technique is employed to reduce the impact of sensor noise and provide high-precision attitude, velocity, and position information for underwater gravity measurement.

Based on the inertial navigation error model, the state variables are selected as:

$$X = [\phi_E \ \phi_N \ \phi_U \ \delta V_E \ \delta V_N \ \delta L \ \delta \lambda \ \varepsilon_x \ \varepsilon_y \ \varepsilon_z \ \nabla_x \ \nabla_y \ \nabla_z]^T \quad (4)$$

The variables  $\phi_E, \phi_N, \phi_U$  correspond to attitude errors, while  $\delta V_E, \delta V_N$  represent eastward and northward velocity errors, respectively. Similarly,  $\delta L, \delta \lambda$  represent the latitude and longitude errors, respectively. The variables  $\varepsilon_x, \varepsilon_y, \varepsilon_z$ , as well as  $\nabla_x, \nabla_y, \nabla_z$ , correspond to gyroscope and accelerometer errors. The system state equation is constructed as follows:

$$\dot{X} = FX + GW \quad (5)$$

In the equations,  $F$  denotes the system state transition matrix,  $G$  signifies the noise driving matrix, and  $W$  represents the system noise. The precise parameters of these matrices are explicated in reference [28].

In underwater scenarios, the EML speed reference information  $v_{refewater}^n$  encompasses the velocity of both the ocean current and the ground simultaneously.

$$v_{refewater}^n = v_{true}^n + \delta v_f + \delta v_\sigma \quad (6)$$

In the equations, the symbol  $v_{true}^n$  denotes the actual ground reference velocity,  $\delta v_f$  represents the ocean current velocity, and  $\delta v_\sigma$  signifies the sensor measurement noise. Presuming that the ocean current velocity  $\delta v_f$  undergoes negligible variations over a short time, subtracting two consecutive EML velocity reference information  $v_{refewater}^n$  values eliminates a significant portion of the ocean current velocity  $\delta v_f$ , leading to the carrier's incremental ground speed.

$$v_{refewater}^n(k) - v_{refewater}^n(k-1) = \Delta v_f^n(k) = v_{true}^n(k) - v_{true}^n(k-1) + \delta v_\sigma \quad (7)$$

In the given equations,  $k$  and  $k-1$  represent consecutive sampling instants whose frequency is determined by the EML data frequency. Likewise, the difference between the ground



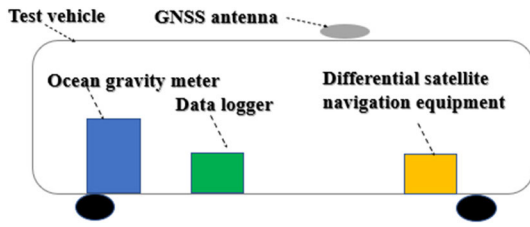


FIGURE 3. Schematic diagram of the experimental equipment installation.

speed  $v_{SINS}^n$  obtained from two consecutive SINS solutions can be calculated:

$$\begin{aligned} \Delta v_{SINS}^n(k) &= v_{SINS}^n(k) - v_{SINS}^n(k-1) \\ &= v_{true}^n(k) - v_{true}^n(k-1) \\ &\quad + \delta v_{SINS}^n(k) - \delta v_{SINS}^n(k-1) + \delta v_{SINS} \end{aligned} \quad (8)$$

$\delta v_{SINS}$  denotes the noise component,  $\delta v_{SINS}^n$  denotes the velocity error of SINS. Subtract  $\Delta v_r^n(k)$  from  $\Delta v_{SINS}^n(k)$ :

$$\begin{aligned} Z(k) &= \Delta v_r^n(k) - \Delta v_{SINS}^n(k) \\ &= \begin{bmatrix} \Delta v_r^E(k) - \Delta v_{SINS}^E(k) \\ \Delta v_r^N(k) - \Delta v_{SINS}^N(k) \end{bmatrix} \end{aligned} \quad (9)$$

The superscripts E and N in the given equations represent the eastward and northward components, respectively, of the corresponding physical quantities. By substituting equations (7) and (8) into equation (9), the measurement equation can be derived.

$$\begin{aligned} Z(k) &= \Delta v_r^n(k) - \Delta v_{SINS}^n(k) \\ &\approx \begin{bmatrix} -\delta v_{SINS}^E(k) \\ -\delta v_{SINS}^N(k) \end{bmatrix} + \begin{bmatrix} \delta v_{SINS}^E(k-1) \\ \delta v_{SINS}^E(k-1) \end{bmatrix} + \delta v \end{aligned} \quad (10)$$

To simplify the construction of the filtering equation, the state equation presented in Equation (5) and the measurement equation described in Equation (10) are transformed into the following forms:

$$\begin{cases} x(n+1) = \phi(n)x(n) + \Gamma(n)u(n) \\ y(n) = H(n)x(n) + N(n)x(n-1) + v(n) \end{cases} \quad (11)$$

In the provided equations,  $n$  denotes the time information,  $x(n)$  denotes the system state,  $\phi(n)$  denotes the system transition matrix,  $\Gamma(n)$  denotes the noise driving matrix,  $u(n)$  denotes the process noise-related quantity,  $y(n)$  denotes the measurement information,  $H(n)$  denotes the observation matrix,  $n(n)$  denotes the delay state matrix, and  $v(n)$  denotes the observation noise. The covariance matrix of  $u(n)$  is  $Q(n)$ , and the covariance matrix of  $v(n)$  is  $r(n)$ . The filtering equation for the delayed state [29] is derived from these equations, including state prediction, prediction of the state covariance matrix, calculation of the filtering gain, measurement update and update of the state covariance, in equations (12) through (16), as shown at the bottom of the next page.

In underwater environments, the velocity information obtained from the EML typically exhibits complex colored noise that varies over time. Moreover, differentiating this

velocity information can lead to high-frequency noise amplification, thereby necessitating adaptive processing of the measurement noise. This study extends the delayed-state filtering equations presented in equations (12) through (16) by incorporating adaptive processing of the measurement noise covariance matrix in equations (17), as shown at the bottom of the next page, where  $\hat{R}(n)$  represents the adaptive measurement noise covariance matrix (replacing  $R(n)$  in equation (14)),  $H(n)$  denotes the observation matrix,  $P(n|n-1)$  denotes the one-step prediction covariance matrix,  $b$  denotes the fading factor, and  $\beta(n)$  denotes the intermediate variable used in the iterative calculation. Generally, the value of  $b$  is tuned between 0.9 and 0.999, with lower values indicating stronger adaptive ability but greater fluctuations in the estimated state. The initial value of  $\beta(n)$ , denoted as  $\beta(0)$ , is typically set to 0.5.  $\beta(n)$  is updated after each measurement update during the filtering process.

### III. EXPERIMENTAL VERIFICATION

Section III aims to demonstrate the effectiveness of the proposed method through experimental verification. Specifically, the on-board test data were utilized to simulate underwater scenarios, and the proposed method was validated through semi-physical simulations.

#### A. EXPERIMENTAL CONDITIONS

In September 2022, the ocean gravity meter, differential satellite navigation equipment, and data logger were installed on a test vehicle in Wuhan, China. Tables 1 and 2 present the primary performance characteristics of the ocean gravity meter and differential satellite navigation equipment, respectively. The vehicle's air conditioning and uninterrupted power supply were employed to maintain the temperature inside the vehicle at 25–30 °C, minimizing the influence of outdoor temperature fluctuations on the ocean gravity meter. The installation schematic of the experimental setup is depicted in figure 3.

The test vehicle underwent dynamic testing on a route with frequent changes in elevation, located on a highway, with a round-trip length of approximately 72 km. The test vehicle continuously drove along the test route, and four gravity measurements were acquired by performing two round trips along the route. Throughout the experiment, efforts were made to maintain a constant speed and direction of the test vehicle, with an average speed of around 40 km/H. The ocean gravity meter recorded inertial data, including specific force and angular motion data, while the differential satellite navigation equipment provided high-precision reference data on position, depth, and velocity. The data were logged by a data logger and used for semi-physical simulation analysis. However, due to the presence of elevated bridges on the test route, occasional satellite signal obstructions occurred, resulting in multiple data losses in the differential satellite navigation equipment. This scenario of data loss was utilized to verify the proposed depth information fusion method.

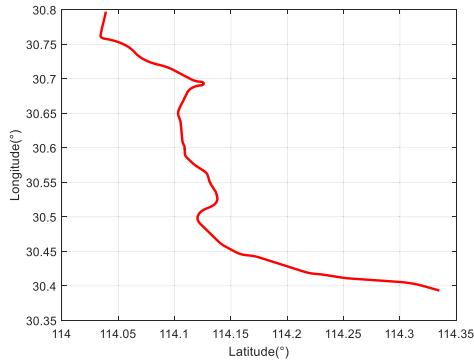


FIGURE 4. Experimental trajectory.

The trajectory of the experiment, depicted in figure. 4, exhibits variations in both longitude and latitude directions, with heading changes exceeding 90°.

**B. SEMI-PHYSICAL SIMULATION DATA PROCESSING**

The method proposed in this study utilizes inertial data obtained from the gravity meter, depth reference data acquired from the differential satellite navigation system, and velocity reference data measured by the EML as inputs to estimate the gravity measurements. However, during the dynamic experiment conducted on the test vehicle, only inertial data and GNSS data were available. Therefore, to evaluate the validity of the proposed method, it is necessary to simulate depth reference data and velocity reference data based on GNSS data. The semi-physical simulation data generation approach is illustrated in the figure 5.

To simulate velocity reference data, errors were introduced to the GNSS velocity data. Since the differential satellite navigation equipment records reference velocity data as ground velocity, simulating underwater EML velocity data requires the addition of underwater current velocity and EML sensor errors to the reference velocity data. (1) Firstly, errors arising from underwater current velocity

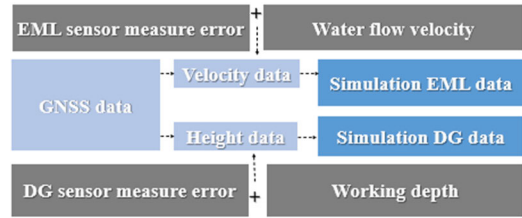


FIGURE 5. Semi-Physical simulation data processing approach.

TABLE 1. Precision indicators of the differential satellite navigation equipment.

Content	Indicators
Horizontal position accuracy (RMS)	≤2.5 cm
Vertical position accuracy (RMS)	≤5 cm
Velocity accuracy (RMS)	≤0.03 m/s

TABLE 2. Precision indicators of the ocean gravity meter.

Content	Indicators
Lunar drift (MAX)	≤5.0 mGal
Static repeatability accuracy (RMS)	≤0.3 mGal
Dynamic repeatability accuracy (RMS, Global Navigation Satellite System (GNSS) supported)	≤1mGal at 0.0033 Hz
Performance of three-axis gyroscope (σ)	≤0.01°/h
Performance of three-axis accelerometer (σ)	Horizontal: ≤20 μg vertical: ≤1 μg

were analyzed. During underwater gravity measurement, diving depths typically exceed 300 m, and in some cases, even reach 2000 m to capture sensitive seabed short-wave gravity information accurately [12], [13], [14], [15]. In the context of autonomous navigation based on inertial/gravity matching for underwater autonomous gravity measurement, covert navigation for submarine platforms is typically conducted at depths exceeding 100 m. At such depths, the impact of conventional ocean winds and waves on underwater current velocity is relatively weak, and the water flow velocity

$$\hat{x}(n|n-1) = \phi(n-1)\hat{x}(n-1|n-1) \tag{12}$$

$$p(n|n-1) = \phi(n-1)p(n-1|n-1)\phi'(n-1) + \Gamma(n-1)Q(n-1)\Gamma'(n-1) \tag{13}$$

$$\begin{cases} S(n) = M_1(n) + M_2(n) \\ M_1(n) = H(n)P(n|n-1)H'(n) + N(n)p(n-1|n-1)N'(n) \\ M_2(n) = N(n)P(n-1|n-1)\phi'(n-1)H'(n) + R(n) + H(n)\phi(n-1)P(n-1|n-1)N'(n) \\ k(n) = P(n|n-1)H'(n)S^{-1}(n) + \phi(n-1)P(n-1|n-1)N'(n)S^{-1}(n) \end{cases} \tag{14}$$

$$\hat{x}(n|n) = \hat{x}(n|n-1) + k(n)[y(n) - H(n)\hat{x}(n|n-1) - N(n)\hat{x}(n-1|n-1)] \tag{15}$$

$$P(n|n) = P(n|n-1) - k(n)[H(n)P(n|n-1) + N(n)P(n-1|n-1)\phi'(n-1)] \tag{16}$$

$$\begin{cases} \hat{R}(n) = (1 - \beta(n))\hat{R}(n-1) + \beta(n)(\hat{Z}(n|n-1)\hat{Z}(n|n-1)^T - H(n)P(n|n-1)H(n)^T) \\ \hat{Z}(n|n-1) = y(n) - H(n)\hat{x}(n|n-1) - N(n)\hat{x}(n-1|n-1) \\ \beta(n) = \frac{1}{n} \sum_{i=0}^{n-1} \frac{\beta(i)}{\beta(i) + b} \end{cases} \tag{17}$$

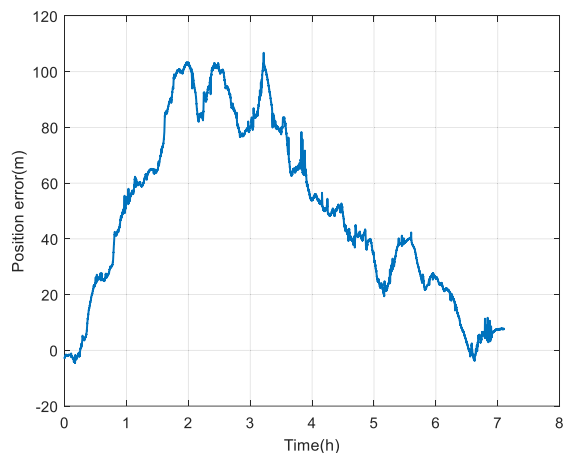


FIGURE 6. Positioning error.

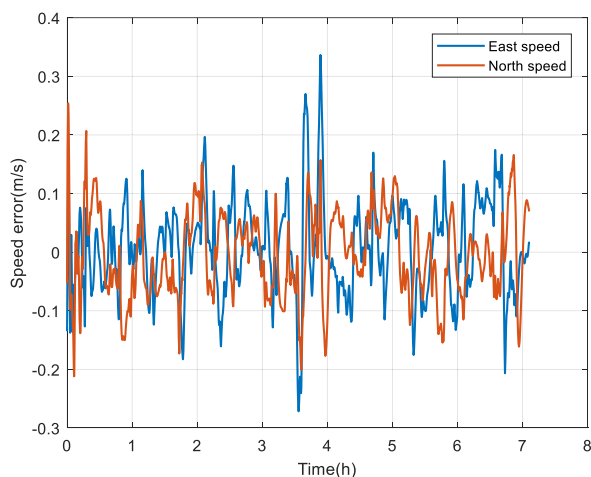


FIGURE 7. Velocity error.

changes very slowly. Therefore, previous research on ocean current velocity was consulted to estimate [30], [31] underwater current velocity as a combination of a constant value and a long-period variation. The constant value was estimated to be 20 cm/s, while the long-period variation was characterized by a period of 11 hours and an amplitude of 3 cm/s. (2) Subsequently, errors originating from the EML sensor were analyzed. By referring to the technical specifications of the commercial EML900 product and considering that the carrier speed during underwater gravity measurement is typically less than 10 knot [10], [11], [12], [13], [14], it can be postulated that the sensor error comprises high-frequency noise and a constant value component. Specifically, the high-frequency noise has an amplitude of 0.2 knot and a standard deviation of 0.1 knot, while the constant value component is 0.2 knot.

To simulate the depth reference data, errors were introduced into the GNSS height data. The differential satellite navigation equipment recorded reference height data with a centimeter level of accuracy, and sensor errors were added to simulate the underwater DG depth data. Assuming a working depth of 2000 m for underwater gravity measurement,

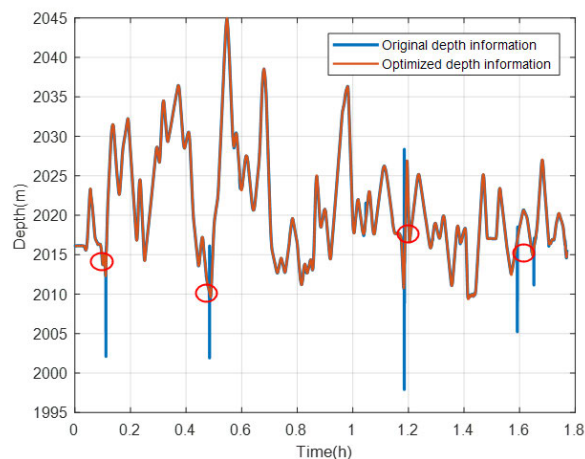


FIGURE 8. Depth information.

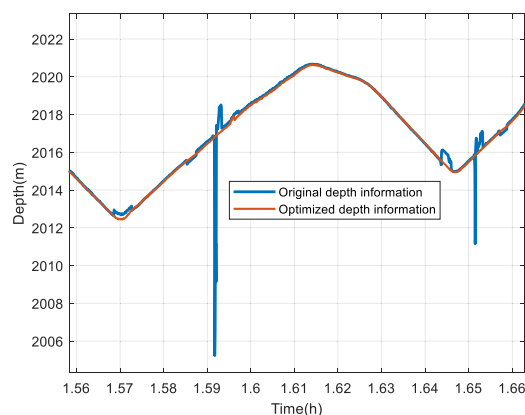


FIGURE 9. Local enlargement of depth information.

the actual working depth was obtained by adding the depth information obtained during the vehicle test to the designed working depth. The DG depth data was then calculated as the sum of the actual working depth and the DG measurement error, estimated as the product of the actual working depth and 0.015%, based on the DG performance specifications [25].

The proposed method for underwater real-time autonomous gravity measurement was validated using inertial data, simulated underwater EML velocity data, and simulated underwater DG depth data. The precision of the method was evaluated using the in-congruence analysis method [32].

### C. EXPERIMENTAL RESULTS

The experimental results, illustrated in figure 6, demonstrate that the maximum positioning error is less than 115 m, indicating significant suppression of water current velocity influence. This suppression provides a reliable positional reference for underwater autonomous gravity measurement. Notably, the proposed methods substantially reduce the rate of divergence in positioning error. The gyroscope accuracy inside the gravimeter is 0.01 °/h, corresponding to an autonomous positioning accuracy of approximately

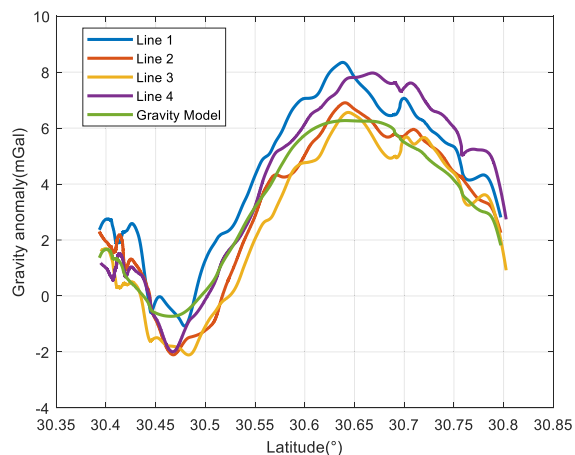


FIGURE 10. Results of repetitive survey lines for gravity measurement.

TABLE 3. In-congruence accuracy within the two survey lines.

accuracy (mGal)	line 1:	line 2:	line 3:	line 4:
line 1:	\	0.63	0.87	0.49
line 2:	\	\	0.52	0.62
line 3:	\	\	\	1.01
gravity model	1.73	0.95	1.24	1.98

1 nautical mile/hour. After adopting the proposed method, with the assistance of external velocity information, the positioning accuracy has been greatly improved, which can meet the needs of gravity measurement.

The velocity error illustrated in figure 7 is 0.072 m/s (RMS) toward the east and 0.077 m/s (RMS) toward the north. These values indicate that the proposed method effectively suppresses the influence of water current velocity by differentially processing EML velocity information. Notably, the stability of the velocity error without divergence as the filtering time increases provides further evidence of the proposed method’s feasibility.

During the repetitive survey lines for gravity measurement, irregularities in the depth information were observed in figure 8 with a local enlargement in figure 9. The blue curve in the circles indicates instances of jumping or missing DG depth reference information at approximately 1.19 H, 0.43 H, and 0.11 H, which were discovered during the survey. The proposed method was able to effectively handle the switching of depth information (indicated by the red curve in the circles). This ensured that there was smooth and continuous depth information, which, in turn, enhanced the accuracy of the vertical motion acceleration calculation.

Based on the global gravity field model released by Professor Sandwell in 2014 [17], gravity data corresponding to the position information of the survey line is extracted and evaluated for the measured gravity results. The global gravity field model can accurately describe the trend of longwave gravity changes, but cannot describe shortwave

gravity changes. Therefore, the global gravity field model can be used to evaluate the trend of measured gravity results. Considering that the constant correction does not affect the trend of gravity changes, for the convenience of comparison, we have superimposed the constant correction on the global gravity field model, and the data comparison curve is shown in the figure 10.

The measured gravity results have the same trend as the global gravity field model, indicating the rationality and feasibility of the proposed gravity measurement method. Moreover, as the measured gravity results come from onboard gravity tests, and can reflect shortwave gravity information. The global gravity field model uses satellite gravity as the data source, mainly reflecting longwave gravity information. Therefore, the measured gravity results can describe the details of gravity changes that cannot be described by global gravity field models. The analysis of the accuracy of in consistency between any two survey lines is presented in Table 3, where the in-consistency accuracy within the competitive survey lines is 1.01 mGal at 0.0033 Hz, and the out-congruence accuracy between the gravity model and survey lines is 1.98 mGal at 0.0033 Hz.

#### IV. DISCUSSION

Upon application of the proposed method, the positioning error exhibits long-period fluctuations. This is attributed to the inability of differential processing of adjacent velocity reference information to eliminate the influence of underwater ocean currents. As the survey time and distance increase, the positioning error gradually increases, which poses limitations on long-duration autonomous underwater gravity measurement. However, it is important to note that gravity measurement is not sensitive to positioning error, and a positioning accuracy of 1852 m suffices to meet the mGal-level underwater gravity measurement requirements [14]. Moreover, during navigation, position calibration can be achieved using inertial/gravity-matching navigation, thereby establishing a beneficial feedback loop.

In situations where the carrier maintains a constant depth during the survey, the DG measurement error is mainly characterized by a constant relative depth error. Considering the measurement error of DG sensor products at a water depth of 2000 m, which is approximately 0.3m, this results in a gravity measurement error of about 0.1 mGal (where a 1m depth error leads to a normal gravity correction error of 0.309 mGal). However, when the carrier’s depth fluctuates considerably, the DG measurement error becomes coupled with the carrier’s depth changes, resulting in low-frequency motion acceleration that is challenging to eliminate. Thus, limiting the carrier’s maneuverability can significantly enhance the accuracy of underwater gravity measurements.

#### V. CONCLUSION

Underwater gravity measurement technology currently focuses primarily on gravity mapping and often relies on



supplementary tools, such as DVL, acoustic positioning, or even mother ship towing. However, these methods have limitations in autonomy, as they require signal emission or the pre-deployment of response signal base stations. In contrast, inertial/gravity-matching navigation requires high autonomy for long-duration and covert underwater navigation. Thus, current underwater gravity measurement technology lacks the autonomy required to meet the demands of autonomous navigation with inertial/gravity-matching.

This study proposes a real-time autonomous gravity measurement method suitable for underwater gravity-assisted navigation to address the challenges mentioned earlier. The proposed method integrates a gravimeter, EML, and DG to provide essential information, such as inertial, positional, velocity, depth, and motion acceleration required for gravity measurement. By combining these sensors, the proposed method enables real-time autonomous underwater gravity measurement. The proposed method aims to provide high-precision navigation information and minimize the impact of water flow velocity. It achieves this goal through a gravimeter/EML fusion navigation method that uses adaptive delay state filtering of measurement noise. In addition, the proposed method enhances the accuracy of vertical motion acceleration measurement by utilizing a depth information processing method that fuses gravimeter and DG data. The effectiveness of the proposed method was verified by utilizing vehicle test data and simulation data from semi-physical underwater environment experiments. The results demonstrate that the proposed method's accuracy within repetitive survey lines is superior to 1.01 mGal at 0.0033 Hz.

The beneficial effects of the proposed method include two aspects: (1) it does not rely on external radio navigation aids and provides gravity information through autonomous measurement, meeting the requirements of gravity matching navigation; (2) It does not include time-consuming data processing and can provide real-time gravity information to meet the real-time application requirements of gravity matching navigation.

In the future, the proposed method will be validated by carrying out underwater gravity measurement experiments with unmanned aerial vehicles.

## REFERENCES

- [1] Y. Bidel, N. Zahzam, C. Blanchard, A. Bonnin, M. Cadoret, A. Bresson, D. Rouxel, and M. F. Lequentrec-Lalancette, "Absolute marine gravimetry with matter-wave interferometry," *Nature Commun.*, vol. 9, no. 1, pp. 627–636, Feb. 2018.
- [2] M. Gilardoni, M. Reguzzoni, and D. Sampietro, "GECO: A global gravity model by locally combining GOCE data and EGM2008," *Studia Geophysica Geodaetica*, vol. 60, no. 2, pp. 228–247, Apr. 2016.
- [3] A. V. Motorin and A. S. Nosov, "Accuracy and sensitivity analysis for marine gravimetry algorithms in dependence of survey conditions," in *Proc. IEEE Conf. Russian Young Researchers Electr. Electron. Eng. (EICoNus)*, Saint Petersburg Moscow, Russia, Jan. 2019, pp. 1210–1215.
- [4] M. Przyborski, J. Pyrchla, K. Pyrchla, and J. Szulwic, "MicroGal gravity measurements with MGS-6 Micro-G LaCoste gravimeter," *Sensors*, vol. 19, no. 11, pp. 2592–2602, Jun. 2019.
- [5] A. A. Golovan, V. V. Klevtsov, I. V. Koneshov, Y. L. Smoller, and S. S. Yurist, "Application of GT-2A gravimetric complex in the problems of airborne gravimetry," *Izvestiya, Phys. Solid Earth*, vol. 54, no. 4, pp. 658–664, Jul. 2018.
- [6] A. V. Sokolov, A. A. Krasnov, and L. K. Zheleznyak, "Improving the accuracy of marine gravimeters," *Gyroscopy Navigat.*, vol. 10, no. 3, pp. 155–160, Jul. 2019.
- [7] Z. Zhuoyang, W. Bin, H. Tiantian, and S. Kaichen, "A fusion algorithm of underwater dual-sensor gravimeter," *IEEE Sensors J.*, vol. 22, no. 1, pp. 461–471, Jan. 2022.
- [8] T. Ishihara, M. Shinohara, H. Fujimoto, T. Kanazawa, A. Araya, T. Yamada, K. Iizasa, S. Tsukioka, S. Omika, T. Yoshiume, M. Mochizuki, and K. Uehira, "High-resolution gravity measurement aboard an autonomous underwater vehicle," *Geophysics*, vol. 83, no. 6, pp. 119–135, Nov. 2018.
- [9] J. Wang, Y. Fang, and X. Meng, "A joint inversion algorithm for the establishment of high-accuracy 3-D marine gravity field," *IEEE Trans. Geosci. Remote Sens.*, vol. 60, 2022, Art. no. 4205013.
- [10] T. Ishihara, M. Shinohara, A. Araya, T. Yamada, T. Kanazawa, K. Uehira, M. Mochizuki, H. Fujimoto, S. Tsukioka, S. Omika, T. Yoshiume, and K. Iizasa, "Development of an underwater gravity measurement system with autonomous underwater vehicle for marine mineral exploration," in *Proc. Techno-Ocean*, Kobe, Japan, Oct. 2016, pp. 127–133.
- [11] M. Shinohara, T. Kanazawa, H. Fujimoto, T. Ishihara, T. Yamada, A. Araya, S. Tsukioka, S. Omika, T. Yoshiume, M. Mochizuki, K. Uehira, and K. Iizasa, "Development of a high-resolution underwater gravity measurement system installed on an autonomous underwater vehicle," *IEEE Geosci. Remote Sens. Lett.*, vol. 15, no. 12, pp. 1937–1941, Dec. 2018.
- [12] L. V. Kiselev, A. V. Medvedev, V. B. Kostousov, and A. E. Tarkhanov, "Autonomous underwater robot as an ideal platform for marine gravity surveys," in *Proc. 24th Saint Petersburg Int. Conf. Integr. Navigat. Syst. (ICINS)*, Saint Petersburg, Russia, May 2017, pp. 1–4.
- [13] Z. Zhang, Z. Liu, and H. Zhang, "Underwater mobile gravity measurement data processing using continuous-discrete Kalman filter," *AIP Adv.*, vol. 11, no. 8, Aug. 2021, Art. no. 085104.
- [14] Z. Xiong, J. Cao, M. Wu, S. Cai, R. Yu, and M. Wang, "A method for underwater dynamic gravimetry combining inertial navigation system, Doppler velocity log, and depth gauge," *IEEE Geosci. Remote Sens. Lett.*, vol. 17, no. 8, pp. 1294–1298, Aug. 2020.
- [15] Z. Xiong, M. Wu, J. Cao, Y. Liu, R. Yu, and S. Cai, "An underwater gravimetry method using inertial navigation system and depth gauge based on trajectory constraint," *IEEE Geosci. Remote Sens. Lett.*, vol. 18, no. 9, pp. 1510–1514, Sep. 2021.
- [16] P. Zingerle, R. Pail, T. Gruber, and X. Oikonomidou, "The combined global gravity field model XGM2019e," *J. Geodesy*, vol. 94, no. 7, pp. 66–78, Jul. 2020.
- [17] D. T. Sandwell, R. D. Müller, W. H. F. Smith, E. Garcia, and R. Francis, "New global marine gravity model from CryoSat-2 and Jason-1 reveals buried tectonic structure," *Science*, vol. 346, no. 6205, pp. 65–67, Oct. 2014.
- [18] Y. Han, B. Wang, Z. Deng, S. Wang, and M. Fu, "A mismatch diagnostic method for TERCOM-based underwater gravity-aided navigation," *IEEE Sensors J.*, vol. 17, no. 9, pp. 2880–2888, May 2017.
- [19] Z. Yang, Z. Zhu, and W. Zhao, "A triangle matching algorithm for gravity-aided navigation for underwater vehicles," *J. Navigat.*, vol. 67, no. 2, pp. 227–247, Mar. 2014.
- [20] Y. Han, B. Wang, Z. Deng, and M. Fu, "A matching algorithm based on the nonlinear filter and similarity transformation for gravity-aided underwater navigation," *IEEE/ASME Trans. Mechatronics*, vol. 23, no. 2, pp. 646–654, Apr. 2018.
- [21] B. Wang, J. Zhu, Z. Deng, and M. Fu, "A characteristic parameter matching algorithm for gravity-aided navigation of underwater vehicles," *IEEE Trans. Ind. Electron.*, vol. 66, no. 2, pp. 1203–1212, Feb. 2019.
- [22] F. Jalal and F. Nasir, "Underwater navigation, localization and path planning for autonomous vehicles: A review," in *Proc. Int. Bhurban Conf. Appl. Sci. Technol. (IBCAST)*, Islamabad, Pakistan, Jan. 2021, pp. 817–828.
- [23] S. Liu, T. Zhang, J. Zhang, and Y. Zhu, "A new coupled method of SINS/DVL integrated navigation based on improved dual adaptive factors," *IEEE Trans. Instrum. Meas.*, vol. 70, pp. 1–11, 2021.
- [24] M. Schilling and O. Gitlein, "Accuracy estimation of the IfE gravimeters Micro-G LaCoste gPhone-98 and ZLS Burriss Gravity Meter B-64," in *Proc. IAG Sci. Assem. (International Association of Geodesy Symposia)*, vol. 143, 2015, pp. 249–256.

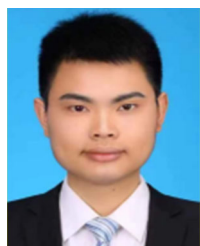
- [25] S. Xiao, M. Zhang, C. Liu, C. Jiang, X. Wang, and F. Yang, "CTD sensors for ocean investigation including state of art and commercially available," *Sensors*, vol. 23, no. 2, pp. 586–608, Jan. 2023.
- [26] Y. Dai, L. Xing, Z. Xiong, R. Wang, and Z. Wan, "The error correction method of the inertial altitude based on air data," in *Proc. IEEE Chin. Guid., Navigat. Control Conf. (CGNCC)*, Nanjing, Aug. 2016, pp. 1393–1397.
- [27] P. Liu, N. Kouguchi, and Y. Li, "Velocity measurement of coherent Doppler sonar assisted by frequency shift, Kalman filter and linear prediction," *J. Mar. Sci. Eng.*, vol. 9, no. 2, p. 109, Jan. 2021.
- [28] S. Du, Y. Huang, B. Lin, J. Qian, and Y. Zhang, "A lie group manifold-based nonlinear estimation algorithm and its application to low-accuracy SINS/GNSS integrated navigation," *IEEE Trans. Instrum. Meas.*, vol. 71, pp. 1–27, 2022.
- [29] V. L. Schwenk, "Algorithms for Kalman filters with delayed state measurements," Ph.D. dissertation, Dept. Elect. Eng., Iowa State Univ., Ames, IA, USA, 1974.
- [30] H.-J. Wagner, K. Kemp, U. Mattheus, and I. G. Priede, "Rhythms at the bottom of the deep sea: Cyclic current flow changes and melatonin patterns in two species of demersal fish," *Deep Sea Res. I, Oceanographic Res. Papers*, vol. 54, no. 11, pp. 1944–1956, Nov. 2007.
- [31] Q. X. Wu and D. Pairman, "A relaxation labeling technique for computing sea surface velocities from sea surface temperature," *IEEE Trans. Geosci. Remote Sens.*, vol. 33, no. 1, pp. 216–220, Jan. 1995.
- [32] W. Wang, J. Gao, D. Li, T. Zhang, X. Luo, and J. Wang, "Measurements and accuracy evaluation of a strapdown marine gravimeter based on inertial navigation," *Sensors*, vol. 18, no. 11, pp. 3902–3915, Nov. 2018.



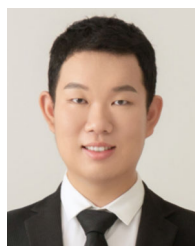
**SHENG ZHONG** received the Ph.D. degree in engineering from the Huazhong University of Science and Technology, in June 2005. He is currently the Vice Dean and a Doctoral Supervisor with the School of Artificial Intelligence and Automation, Huazhong University of Science and Technology. His main research focuses on digital image processing and pattern recognition in the fields of imaging autonomous navigation, imaging automatic target detection, and real-time implementation.



**YUE LENG** is currently pursuing the Ph.D. degree in artificial intelligence and automation with the Huazhong University of Science and Technology, mainly engaged in gravity measurement and gravity matching navigation related work.



**WENYU AI** was born in China, in 1990. He received the M.Sc. degree from the Huazhong Institute of Electro-Optics, Wuhan, China, in 2015. He is currently pursuing the Ph.D. degree in electronic information engineering with the School of Artificial Intelligence and Automation, Huazhong University of Science and Technology. His research interests include navigation, gravity measurement, and instrument engineering.



**SHIBO WANG** received the master's degree from the Beijing University of Aeronautics and Astronautics, in 2019, mainly engaged in gravity measurement and gravity matching navigation related work.

• • •